Characteristic and oscillation tendency study for different seat geometries of the pilot stage of a two-staged pressure control valve

Martin Kloetzer[12]*, Jürgen Weber[1],

[1]*Institute of Mechatronic Engineering, Technische Universität Dresden, Helmholtzstrasse 7a, 01069 Dresden*
[2] *Rausch & Pausch / Albert-Pausch-Ring 1, 95100 Selb, Germany*
* *Corresponding author: Tel.: +49 281/67339; E-mail address: mkloetzer@rapa.com*

ABSTRACT

Two-staged pressure control valves are used in various applications. The usage in semi-active shock absorbers leads to several advantages compared to orifice controlled proportional valves. However, the high dynamic operation and limited assembly space as well as an oscillation tendency requires a detailed understanding and precise layout of the valve, especially the pilot stage. This paper presents a research study of different seat geometries of the pilot stage of a two-staged pressure control valve concerning function parameters and oscillation tendency.

The pilot stage operates as a pressure relief valve with the function to achieve a specific pressure at the pilot seat. The relevant equations to describe the function is the balance of forces combined with the equations of the individual factors (e.g. flow-force). The derivation and determination is done analytically. Just a few parameters, e.g. hydraulic resistance characteristic, will be determined by numerical CFD-simulations and measurements. The relevant description is the pressure-flow-stroke-characteristic (p-Q-x). In general, the study is verified by comparison with measurements and 1D-system simulation.

For pilot stage valves as well as pressure relief valves, there are different possible geometries for the seat and the sealing edge (e.g. ball or cone poppet seat). The various geometries have different advantages and disadvantages regarding performance, stroke dependency, dynamic behaviour as well as component complexity and robustness. This paper demonstrates the impact on different poppet seat geometries regarding the listed factors above. This provides the following benefits: First, simple overview and comparison of various poppet valve concepts regarding basic function. Secondly, a detailed influence analyses of specific design parameters. Additionally, this study can easily be used or extended by the user due to the analytical approach. Finally, this study shows and explains the fundamental functionality and dependencies. This increases the knowledge and application opportunities by helping to design poppet valves.

Keywords: Design Process, Fluids & Tribology, Characteristic and oscillation tendency study, pressure relief valve, geometry-function study of poppet valve design

1. INTRODUCTION

Semi-active shock absorbers are becoming more common within the automotive world. The main requirements on the pressure control valve of the shock absorbers are pressure control accuracy, high dynamic operation and limited packaging. In general, there are two valve types available: direct and pilot operated proportional valve. Direct operated valves or orifice-controlled valves have the advantage of fast dynamics, but the control accuracy of the main piston depends on a high number of

dependencies and component tolerances. This disadvantage is one of the benefits of pilot staged pressure control valves, the control accuracy of the main piston has less dependencies. However, this valve type is more complex in the layout and tends to oscillation at unfavourable operational areas. In sum, two-staged pressure control valve provides advantages and performance once a robust layout without achieved. Therefore, a detailed knowledge and understanding of the relevant characteristic and performance parameters and dependencies are required as well as a comprehension about the valve oscillation tendency.

The two-staged pressure control valve can be separated into 3 sections: main stage, pilot stage and electro-magnetic actor. The main oil flow goes through the main stage. Thereby, the pressure drop will be achieved and controlled. The main piston is not mechanically activated. It is moved by the pressure differences of inlet pressure and counter-control pressure of the pilot stage. This counter-control or pilot stage pressure is created by the pilot stage together with the electro-magnetic actuator, depending on the inlet pressure and the applied current. There are many design options (Valve seat geometries) for the pilot stage of a two-staged pressure control valve available. This paper compares the characteristics of different geometries with an analytical approach and evaluates the oscillation tendency.

2. MECHATRONIC SYSTEM OF THE PILOT STAGE

The pilot stage of a two-staged pressure control valve acts as a pressure relief valve depending on the applied current of the electro-magnet. This system can be described as a mechatronic system and the interference and dependencies can be seen in **Figure 1**:
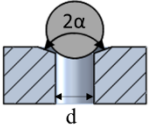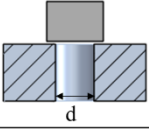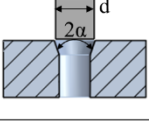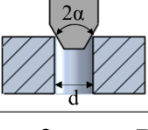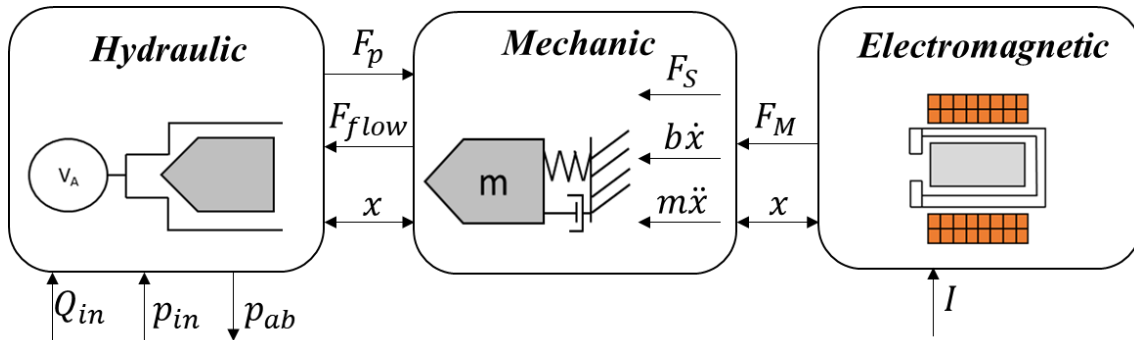

Figure 1: Mechatronic system of a pilot stage

The subsystems of the mechatronic system are Mechanic, Hydraulic and Electro-magnetic. The interaction of those subsystems provides the functionality of the pilot stage: to achieve a certain pressure drop at the valve seat depending on the applied electric current. In the following sections the system equations will be described.

2.1. Hydraulic subsystem

The hydraulic system of the pilot stage is typically a valve seat or metering edge with a chamber volume in front of the seat. As mentioned before, different geometries are possible and will be analysed and compared in this paper. These various geometries define the static and dynamic performance. **Figure 2** shows the different geometries, which will be evaluated:

2

Geometry	Form description
	Seat piece: ball Metering edge: coned edge Cone angle α: 70°
	Seat piece: cylindrical plunger Metering edge: sharp edge
	Seat piece: cylindrical plunger Metering edge: coned edge Cone angle α: 20° & 40°
	Seat piece: coned plunger Metering edge: sharp edge Cone angle α: 40°

Figure 2:   Different valve seat geometries

For this paper, initial pressure area and therefore the diameter d is considered as identical for all geometries. Due to the pressure in the pilot stage inlet chamber, a pressure force on the valve seat piece results, which can be described as in equation (1):

$$F_p = A_p p \tag{1}$$

The pressurized area is dependent on the geometry. For some geometries, the area and stroke interference are a square equation. However, as described in [1], the stroke x for those valves is typically much smaller than seat diameter d. Therefore, the square term is negligible and leads to a linear description of the pressurized area depending on the stroke x:

$$A_p = G_1 + G_2 x \tag{2}$$

Hereby, G_1 is the pressurized area at the initial position ($x = 0$) and can be calculated with:

$$G_1 = A_p(x = 0) = \frac{\pi}{4} d^2 \tag{3}$$

The parameter G_2 describes the linearized factor for the change of the area depending on the stroke, referring to the equation (4):

$$G_2 = \frac{A_p(x) - A_p(x = 0)}{x} \tag{4}$$

The same procedure is applicable for the flow area, which is the cross section between the metering surface and the seat part surface (e.g. coned plunger surface). Therefore, the quadratic term of the stroke x can be neglected and the equation simplified to:

$$A_{flow} = \pi d \sin(\alpha) x = G_3 x \tag{5}$$

This flow area is relevant regarding the flow forces. Those occurs due to the static pressure because of the velocity or the change of the volume flow. This connection is described by Bernoulli's equation and impulse balance [2] which leads to the following equation for the flow force:

$$F_{flow} = k_{GF} \frac{\rho Q^2}{A_{flow}} \tag{6}$$

As mentioned earlier the flow area is dependent on the valve seat geometries. Same applies for the flow coefficient k_{GF}. Typically, the approach is to minimize the occurring flow forces. In this approach the transient term of the flow force is neglected.

Another relevant influence factor is the hydraulic resistance characteristics of the valve seat. Generally, the pressure difference due to a hydraulic resistance is described by the equation (7):

$$\Delta p = \zeta \frac{\rho}{2 A_{flow}^2} Q^2 \tag{7}$$

Therefore, the resistance coefficient ζ is dependent on several factors (e.g. the viscosity of the fluid, or flow Q) and is usually in the literature characterized as function of the Reynolds number Re and the two constants K_1 and K_2 (8). As seen in the equation (9) of the Reynolds number Re, the influence of the viscosity and therefore the temperature is included.

$$\zeta(Re) = \frac{K_1}{Re} + K_2 \tag{8}$$

$$Re = \frac{Q\, d_h}{A_{flow}\, v} \tag{9}$$

The hydraulic diameter d_h is supposed to be proportional to the stroke x [1] and can be described with the perimeter of the flow area P, by the equation (10):

$$d_h = \frac{4\, A_{flow}}{P} \tag{10}$$

The three geometrical factors G$_1$, G$_2$ and G$_3$, mentioned in the equations (3, 4) and (5) as well as ζ will be compared to each other in this paper.

Inserting the equations (8), (9) and (10) into (7) results to the familiar pressure equation:

$$\Delta p(x, Q) = \frac{K_1 \rho v}{2 d_h(x) A_{flow}(x)} Q + \frac{K_2 \rho}{2 A_{flow}(x)^2} Q^2 \tag{11}$$

The resulting pressure difference is mainly dependent on the stroke x and the flow Q. Additionally, the laminar (linear Q-share) and the turbulent (square Q-share) is quite obviously in the equation (11). Another relevant equation is the pressure build-up description within the inlet volume V_A:

$$\dot{p} = \frac{K}{V_A}\left(Q_{in}(t) - Q_{ab}(t)\right) \tag{12}$$

2.2. Electromagnetic subsystem

Pressure control valves in both versions, direct and piloted controlled, are typically activated by an electromagnetic actuator. Sometimes a reset spring is also implemented into the system. The function is to provide an actuating force on the main piston or the pilot valve seat. The electromagnetic characteristic is very depending on the stroke and remanence gap to the pole part. This is described by the force-stroke curve and is dependent on the layout and design of the magnetic circuit system. It could also be adapted with a compression spring. In general, the overall magnetic force stroke gradient cannot be changed. Therefore, just the operational area of the magnetic actuator should be evaluated and adapted. However, there are three different causes for the operational area: Negative (1), horizontal (2) and positive (3) magnetic force gradient over stroke, which are shown in **Figure 3** in a linear schematic model:
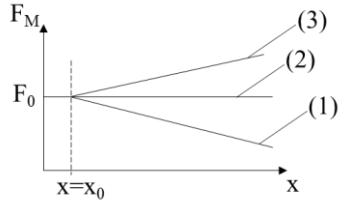
Figure 3: Schematic (linear) model for the magnetic force over stroke curves

The three versions are different in the design and layout. Usually, the magnetic force gradient is manipulated by the magnetic conductance through a pole stage. Considering a starting point at the operation range of the electromagnetic actor at $x = 0$, the initial magnetic force is F_0. The curve of the magnetic force is presumed as a linear behavior, which results in the following equation (13):

$$F_M(I, x) = F_{0,M}(I, x = 0) + c_M x \tag{13}$$

Therefore, the different gradients of raising or falling curve will be described through the sign of c_M. Electromagnetic hysteresis and friction effects are not taken into account. The design with a negative gradient provides the least complex design. This could lead to a commercial benefit in industrial application. The impact on the performance and oscillation tendency will be analyzed within this paper.

2.3. Mechanic subsystem

In some pressure relief valve and also pilot stage system a compression spring for a supporting force and reset-function is used. In this case the spring force and the spring stiffness have a similar behavior as the magnetic force:

$$F_S(x) = F_{0,S}(x = 0) + c_S x \tag{14}$$

Usually in those valve applications, the spring force is the opposite direction of the magnetic force. Therefore, both equation (13) and (14) can be combined into (15):

$$F_{Res}(I, x) = F_{0,Res}(I, x = 0) + (c_M + c_S)x \tag{15}$$

In addition to the spring force, friction and inertial forces are part of the system and need to be considered.

2.4. Complete dynamic mechatronic system

Summing up the shown and explained equations and relations results into the following force balance of the complete dynamic mechatronic system (16):

$$m\ddot{x} + b\dot{x} + F_0 + (c_S + c_M)x + k_{GF}\frac{\rho(Q)^2}{G_3 x} - (G_1 + G_2 x)p = 0 \tag{16}$$

The relevant force scheme with the example of a ball valve seat can be seen in **figure 4**:
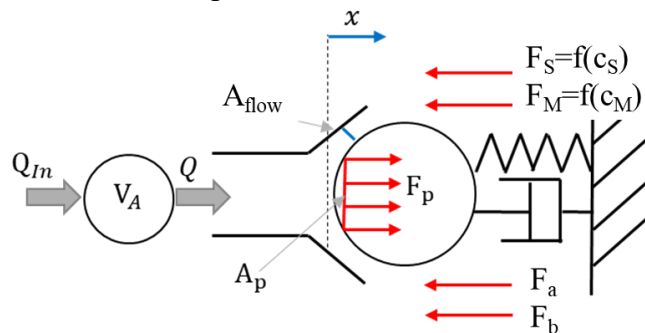
Figure 4: Schematic physical force and influence parameter model of the pilot stage seat

The focus of the paper is the comparison of various geometries and their influence on the mentioned function equation. Hereby the analytical derivation will not be shown in detail and based mainly on [1, 3, 4, 5]. For the following approach the system of the three equations, (16) together with (7) and (12) will be used. Therefore, in order to solve the initial valve problem. following initial conditions are used [1]:

$$p(t = 0) = p_0 \tag{17}$$

$$x(t = 0) = 0 \tag{18}$$

$$\dot{x}(t = 0) = 0 \tag{19}$$

2.5. Stability evaluation by Routh-Hurwitz method

As mentioned before, the stability behavior of pressure relief valves should be evaluated. A very effective method is the Routh-Hurwitz-method for differential equations in the third order [6]. The analytical derivation is based on [1] and will not be shown in detail in this paper due to limited space. Linearization and assumptions are used in the same way. Only the main steps are mentioned below. The force balance (16) is solved for the pressure:

$$p(x) = \frac{m}{G_1}\ddot{x} + \frac{b}{G_1}\dot{x} + \left(\frac{c_S + c_M}{G_1} - \frac{F_0 G_2}{G_1^2}\right)x + \frac{2F_0 G_3 k_{GF}}{G_1^2}\frac{1}{\zeta(x)}x + \frac{F_0}{G_1} \tag{20}$$

The hydraulic resistance characteristics is kept general for now with $\zeta(x)$. The common simplification of assuming a turbulent behavior is not applied [1]. The equation (20) can be inserted in the pressure build-up equation (12) and describes the reaction of the system to the inlet flow $Q_{in}(t)$:

$$Q_{in}(t) = \frac{V_A m}{G_1 K}\dddot{x} + \frac{V_A b}{G_1 K}\ddot{x} + \frac{V_A}{K}\left(\frac{c_S + c_M}{G_1} - \frac{F_0 G_2}{G_1^2} + \frac{2F_0 G_3 k_{GF}}{G_1^2}\frac{1}{\zeta(x)}\right)\dot{x} + \sqrt{\frac{1}{\zeta(x)}}\sqrt{\frac{2F_0}{\rho G_1}}G_3 x \tag{21}$$

Considering small strokes, the simplification of $\dot{\zeta}(x) = 0$ is applied. Substituted with simple coefficients, the equation can be modified for easier usage of the Routh-Hurwitz method to:

$$Q_{in}(t) = a_3\dddot{x} + a_2\ddot{x} + a_1\dot{x} + a_0 x \tag{22}$$

The Routh-Hurwitz method implies that a system is stable once all coefficients and determinants of the system matrix M (23) are positive [6].

$$M = \begin{pmatrix} a_1 & a_3 & 0 \\ a_0 & a_2 & 0 \\ 0 & a_1 & a_3 \end{pmatrix} \tag{23}$$

The coefficients a_0, a_2 and a_3 cannot become negative considering using valid physical values. The coefficient a_1 can be negative and depends on following parameters:

$$a_1 = (c_S + c_M)G_1 - F_0 G_2 + 2F_0 G_3 k_{GF}\frac{1}{\zeta(x)} \tag{24}$$

Analyzing and evaluating the influence parameters, initial force F_0 and G_1 defines the pressure level and is usually an application related given value. Both parameters c_S and c_M describe the modification of the initial force F_0 regarding the stroke x (e.g. magnetic force gradient over stroke). Additionally, the parameters G_2, G_3, k_{GF} and ζ are dependent on the geometry and will be compared in this paper. An extremely interesting relation of this stability criteria and the general pQ-characteristic of those valve type is mentioned in [1] and is evidently visible, when comparing equation (24) with the following pQ-equation (25):

$$\frac{\delta p}{\delta Q} = \frac{\sqrt{\frac{\rho}{2F_0}}}{G_1^{\frac{3}{2}}G_3\sqrt{\frac{1}{\zeta(x)}}}\left((c_S + c_M)G_1 - F_0G_2 + 2F_0G_3k_{GF}\frac{1}{\zeta(x)}\right) \tag{25}$$

Reviewing both equations (24) and (25), the same term determines the slope and the sign of the equation. Therefore, the simple statement that the pQ-characteristic must be raising in order to achieve valve stability can be determined [1].

The second critical criteria of the Routh-Hurwitz method is the determinant D_2, which may become negative:

$$D_2 = \frac{V_A}{K}\left(\frac{c_S + c_M}{G_1} - \frac{F_0G_2}{G_1^2} + \frac{2F_0G_3k_{GF}}{G_1^2}\frac{1}{\zeta(x)}\right)\frac{V_Ab}{G_1K} - \left(\sqrt{\frac{1}{\zeta(x)}}\sqrt{\frac{2F_0}{\rho G_1}}G_3\right)\frac{V_Am}{G_1K} \tag{26}$$

Especially the hydraulic damping b is an interesting influence parameter, which describes the minimum required hydraulic damping to achieve a stable system [1].


3. VALVE SEAT GEOMETRIES PQX-STUDY

In this section the different geometries are explained and discussed. As introduced and shown in **Figure 2**, the characteristics of five different valve seat configurations (geometry and angle) are evaluated. Following parameters that are listed in **table 1** will be used for illustration purposes of the calculations:

Table 1: List of parameters

| Parameter	Value
Valve seat diameter d	2.7×10^{-3} [m]
Density ρ	850 [kg / m]
Mass m	25×10^{-3} [kg]
Bulk modulus K	14000 [bar]
Inlet chamber volume V_A	10×10^{-3} [m³]
Flow coefficient k_{GF}	0.35 [-]
Initial resulting Force F_0	25 [N]

3.1. Geometrical parameters

Initially, the geometrical parameters of the different geometries G_1, G_2, and G_3 are calculated and compared. The first geometrical influence parameter is G_1, which can be calculated with equation (3). Considering the same resulting force F_0, the same pressure operation level and the same diameter d for all geometries, G_1 is identical. For the parameter G_2 the equation (4) can be used. The different behavior for G_2 of the designs can be seen in **Figure 5**:
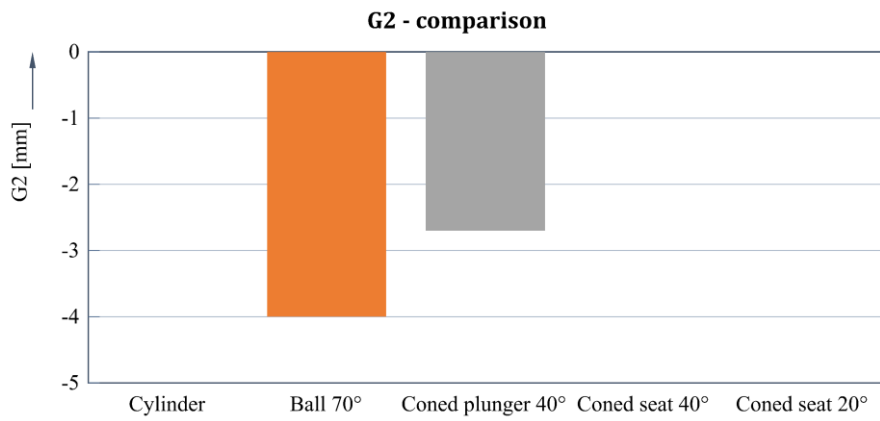
Figure 5: G_2 comparison of the various geometries

Cylinder and coned seat geometries are independent of the stroke. The ball and coned plunger variant decrease the pressurized area with an increasing stroke. The third geometrical parameter G_3 can be calculated with (5) and describes the change of the flow cross section based on the stroke x.
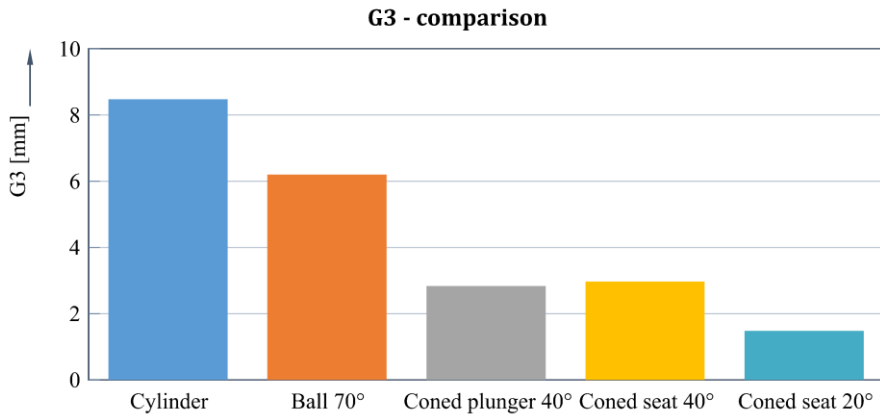

Figure 6: G_3 comparison of the various geometries

Again, the differences between the various geometries are visible.

3.2. PQx-characteristics of the different geometries

The pQx-characteristic is the first step to evaluate and compare the function behaviour of the different geometries for the pilot stage. It shows the resulting pressure difference before and after the pilot stage depending on the flow Q and stroke x. In general, there are four different ways to determine the pQx-curves: CFD-Simulation, measurement on prototypes, via analytical calculation or system-simulation. The last two approaches require reference values for $\zeta(x)$, therefore those are just applicable for recalculation or adaption of existing experience values.
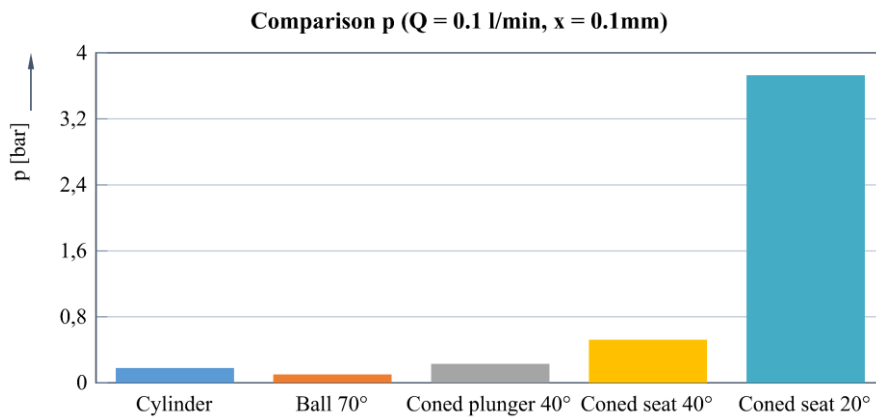
For this paper, CFD-Simulations are used. Below in **Figure 7** the pQx for the ball valve seat is depicted as an example.
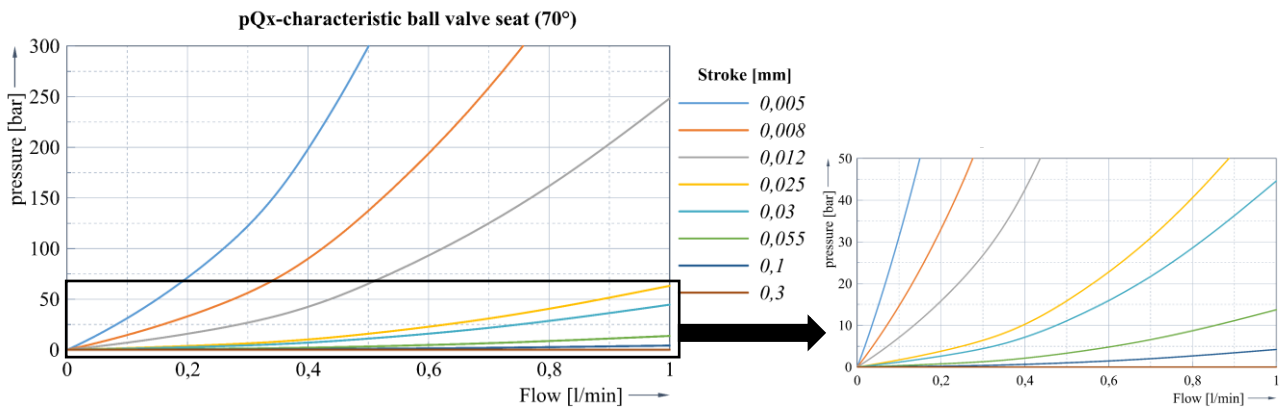
Figure 7: PQx- characteristic for ball valve seat (CFD-Simulation)

Interesting is the comparison of the characteristics for the different geometries. For illustrative purposes following operation point is used: $Q = 0.1\frac{l}{min}$ and $x = 0.1mm$:

Figure 8: $p\left(Q = 0.1\frac{l}{min}, x = 0.1mm\right)$ comparison

Secondly, the operation point of $Q = 0.5\frac{l}{min}$ and a stroke of $x = 0.03mm$ is used for comparison and shown in the **Figure 9** below:
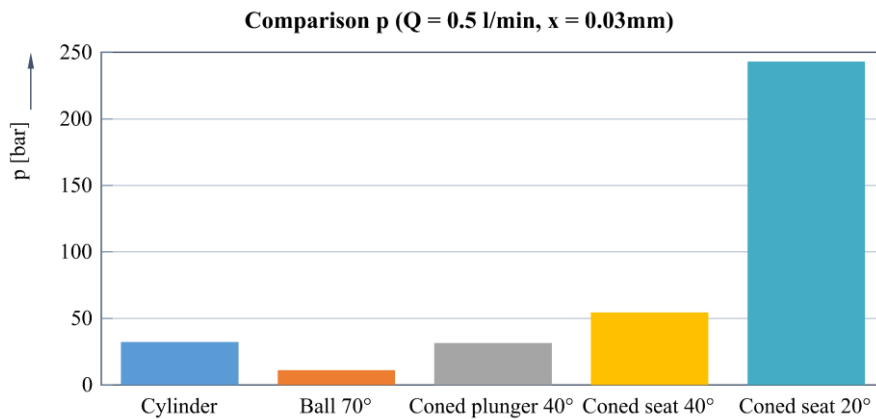
**Figure 9:** $p\left(Q = 0.5\frac{l}{min}, x = 0.03mm\right)$ comparison

It is visible that the coned seat design, especially with the 20°-angled cone achieve a quite high pressure drop.
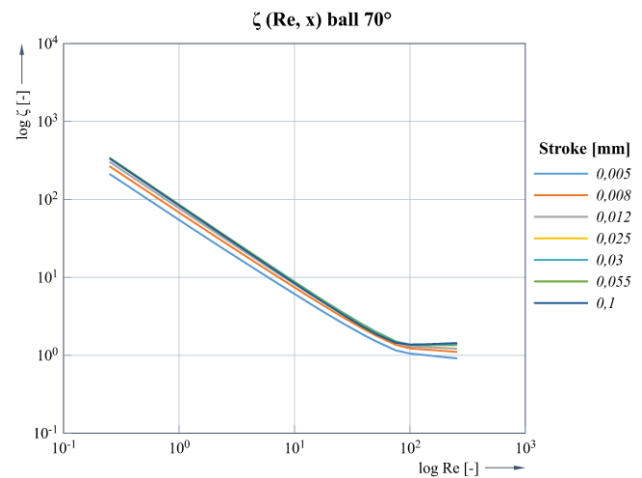
3.3. Hydraulic resistance

In the case of a new investigation or new design, the $\zeta(x)$ must be approximated from simulated or measured pQx-characteristic. Therefore, the equation (7) can be used by solving it for the hydraulic resistance $\zeta(x)$ and converting into a function of the Reynolds number $Re(x)$ (27):

$$\zeta(x, Re) = \Delta p(x) \frac{2}{\rho} \frac{A_{flow}(x)^2}{Q^2} = \frac{K_1(x)}{Re(x)} + K_2(x) \tag{27}$$

Below the characteristics of the $\zeta(x, Re)$ is shown for the examples of the cylinder (**Figure 10**) and ball (**Figure 11**). First, the laminar (linear) and the turbulent (square) share is quite obviously in the double-logarithm display. Second, the difference between both geometries in terms of quantity of the hydraulic resistance. Third, the fluctuation regarding the stroke is visible. The last mentioned, is important to consider, because the calculation of one operation point is not equal to the complete operation range and results can be different, especially with a big value band of $\zeta(x)$ (e.g. cylinder geometry).
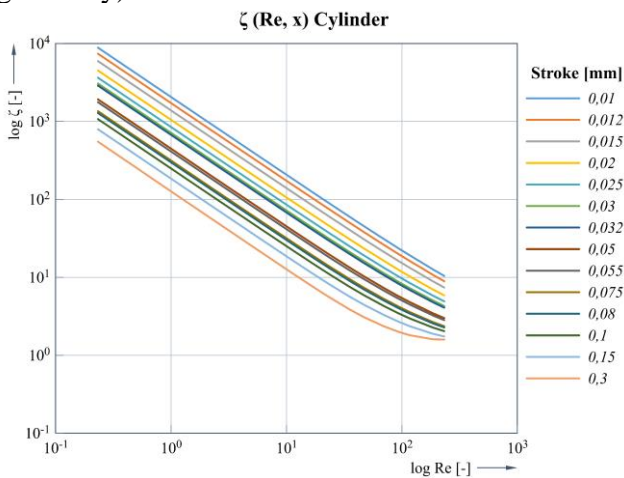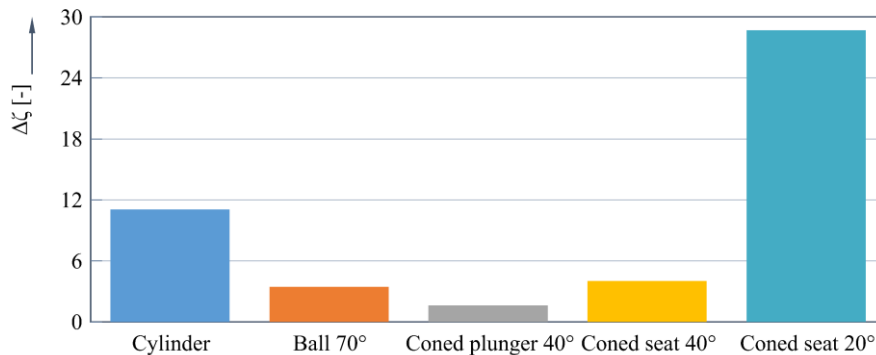

Figure 10: $\zeta(Re, x)$ for the cylinder valve seat geometry

**Figure 11:** $\zeta(Re, x)$ for the ball valve seat geometry

Again, the results for the different geometries should be compared. First, the comparison of the hydraulic resistance is depicted at the operation point of $Q = 0.1 \frac{l}{min}$ and a stroke of $x = 0.1 mm$ (**Figure 12**):

Figure 12: $\zeta(Q, x)$ comparison for the various geometries

Secondly, the width of the band of ζ depending on the stroke at the point of a Reynolds number of 10 is evaluated (**Figure 13**) and shown in the pictures below:
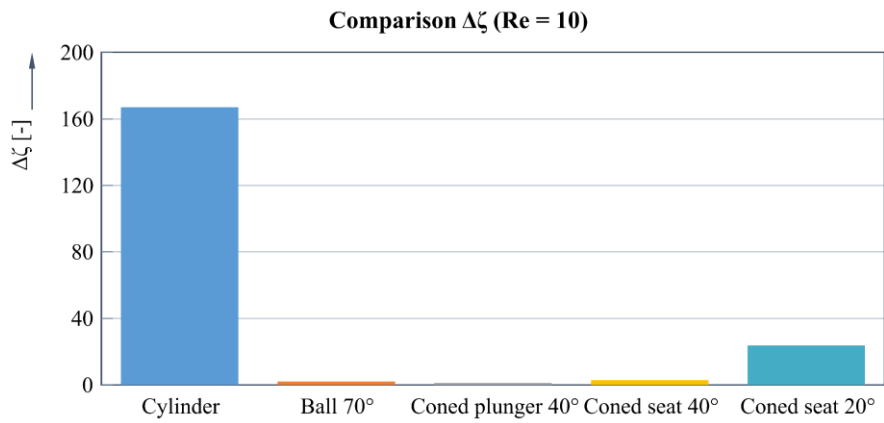
Comparison Δζ (Re = 10)

Figure 13: $\zeta(Re = 10)$-width comparison for the various geometries

The cylinder shows a big band in difference to ball and coned plunger, which shown almost no stroke dependency.

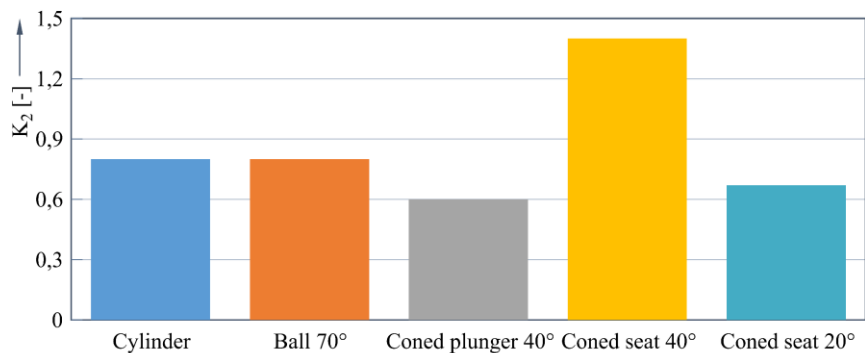From here on, a stroke of $x = 0.1mm$ will be used as reference and boundary condition for further investigations. Therefore, the different values for $K_1(x = 0.1mm)$ and $K_2(x = 0.1mm)$ for the geometries can be determined and compared.

Comparison K$_1$ (x = 0.1mm)
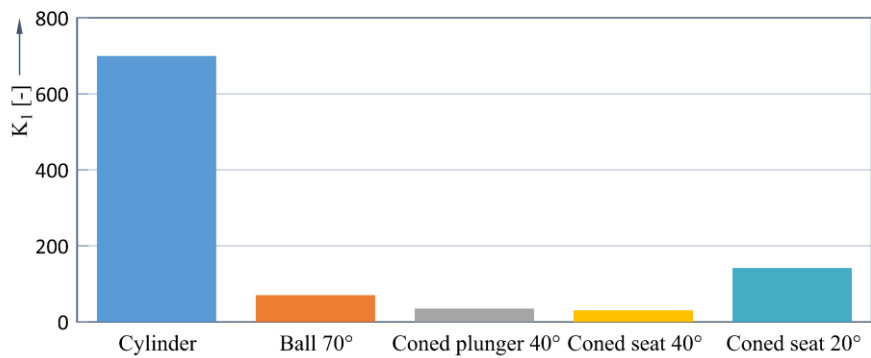
Figure 14: K$_1$ comparison for the various geometries


Comparison K$_2$ (x = 0.1mm)

Figure 15: K$_2$ comparison for the various geometries

3.4. Validation

While using this reference point, an analytical calculation of the pQx-behaviour can be done. This bases on the, from the CFD-approximated, hydraulic resistance characteristic. Due to the limited space, just the pQx-characteristic of the ball seat geometries will be presented in this paper as an example. In the following **Figure 16**, the four curves from the different methods are shown:
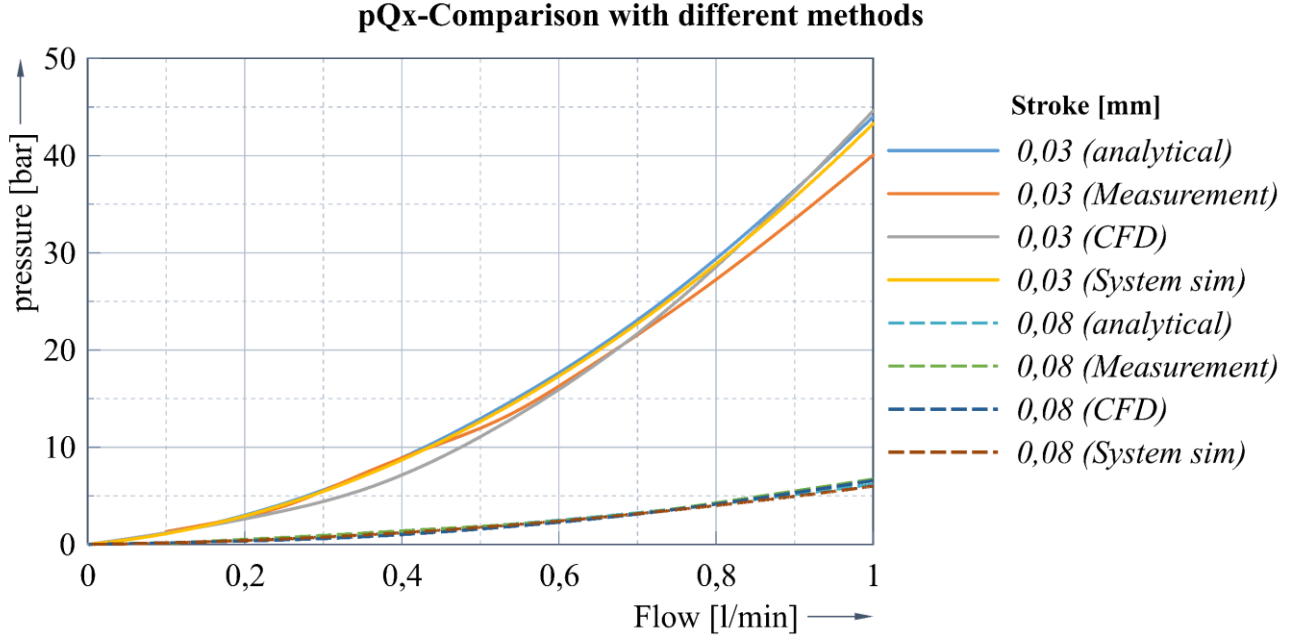

Figure 16: pQx comparison for different methods

The measurements are performed on a hydraulic test bench with a simplified test setup. The stroke of the valve is manually adjusted to the target value for each measurement point. Afterwards the resulting pressure drop based on the flow is measured statically for each operational point. Comparing the curves, all four methods show similar results. That means that the "by-hand" calculation together with approximated values for ζ is accurate enough and can simplified to speed up variant derivations and estimations, if the principial behavior is not changed too much for the reference point.

4. OSCILLATION TENDENCY STUDY

In section 2.5 the stability evaluation method was described with the two requirements that a_1 and D_2 must be positive. Now, this will be used to compare the different geometries by quantifying the oscillation tendency for a pressure relief valve.

First, we will have a look at the a_1 criteria. Reviewing equation (24) the influence parameters are clear and visible. Especially the influence of the amount and the sign of the investigated geometrical parameters can be seen. Examples that have a negative G_2 or a small hydraulic resistance are beneficial. As shown in the section before, there are significant differences between the geometries. The only undefined parameters within the system and the equation (24) are the stiffnesses ($c_S + c_M$). Those depends on the design of the electromagnetic actuator and the mechanic system. The magnetic force gradient is in principle negative; however, it can be tuned by design features (e.g. pole stage) to a horizontal or even positive curve. Those design options require a detailed magnetic field layout, usually done with FEM magnetic force simulations. Additionally, those tuning actions lead to more complex components and higher tolerance dependences, especially relevant for high-volume industrial applications. The sum of the resulting force of the electromagnetic can be adapted by a compression spring.

Initially, the basic version without any pole stages or springs and a magnetic force gradient of -40N/mm will be used as an example. The resulting values for a_1 are shown in **Figure 17**:

Comparison a₁ (c = -40 N/mm)
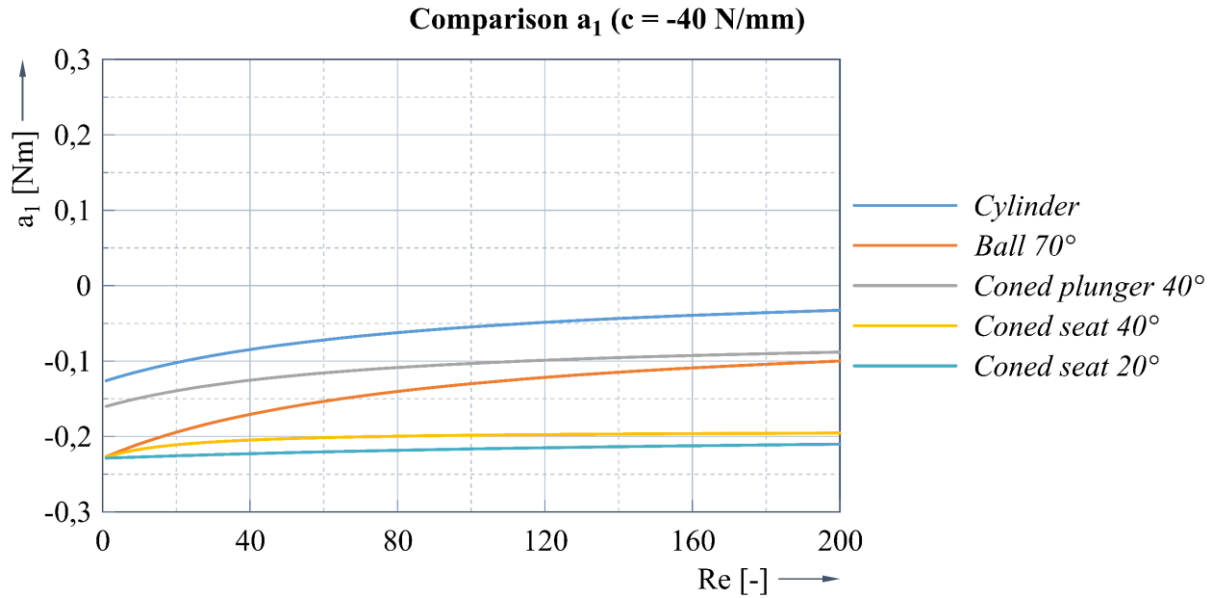
Figure 17: $a_1(c = -40 \frac{N}{mm})$ comparison for the various geometries

As depicted the results for of all geometries a_1 is negative, which would mean that valve configuration would tend towards oscillation. However, different values for the geometries can be detected. For more precise research, equation (24) can be solved for the stiffness and with that a critical force gradient – the minimum required valve to fulfill the stability criteria can calculated and is depictured in **Figure 18**:
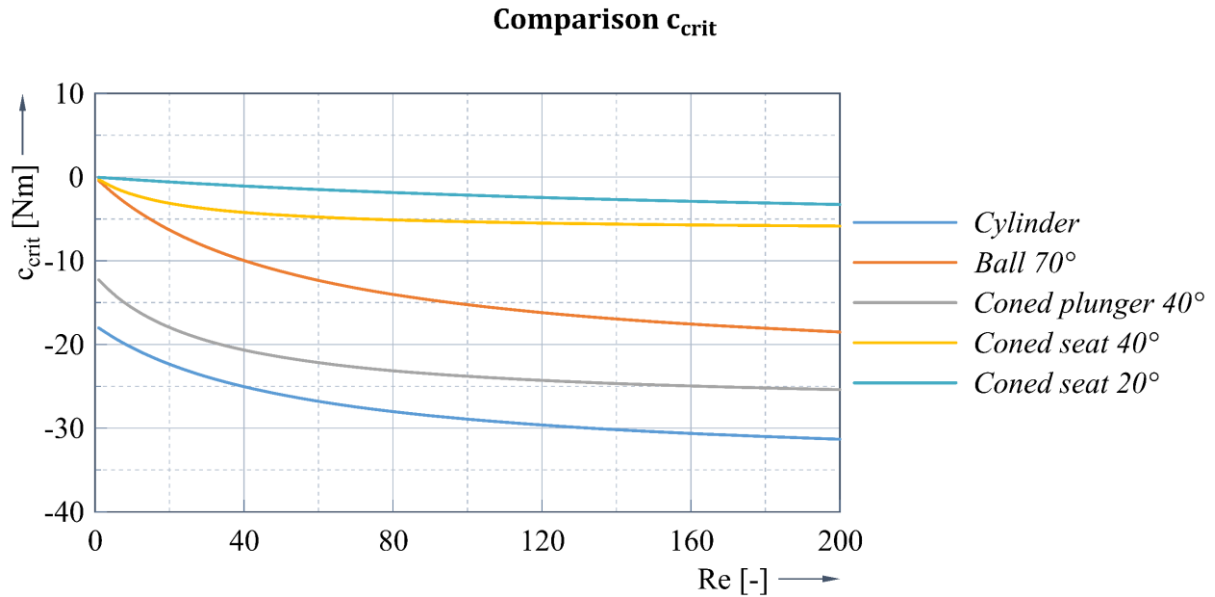
Comparison c_crit

Figure 18: c_{crit} comparison for the various geometries

The ball geometry requires the lowest and the coned geometries the highest minimum magnetic force gradient to fulfill the criteria ($a_1 > 0$). This could be a significant influence parameter to evaluate the layout of electromagnetic actuators, especially in regards of design complexity (e.g. pole stages). Considering the criteria fulfillment for all the geometries at least a horizontal gradient is required ($c_S + c_M = 0$). This kind of parameter influence study can be done extremely fast and easy with the analytically approach, while using the calculation template with. The results are shown in the **Figure 19** below:

13

Comparison a₁ (c = 0 N/mm)
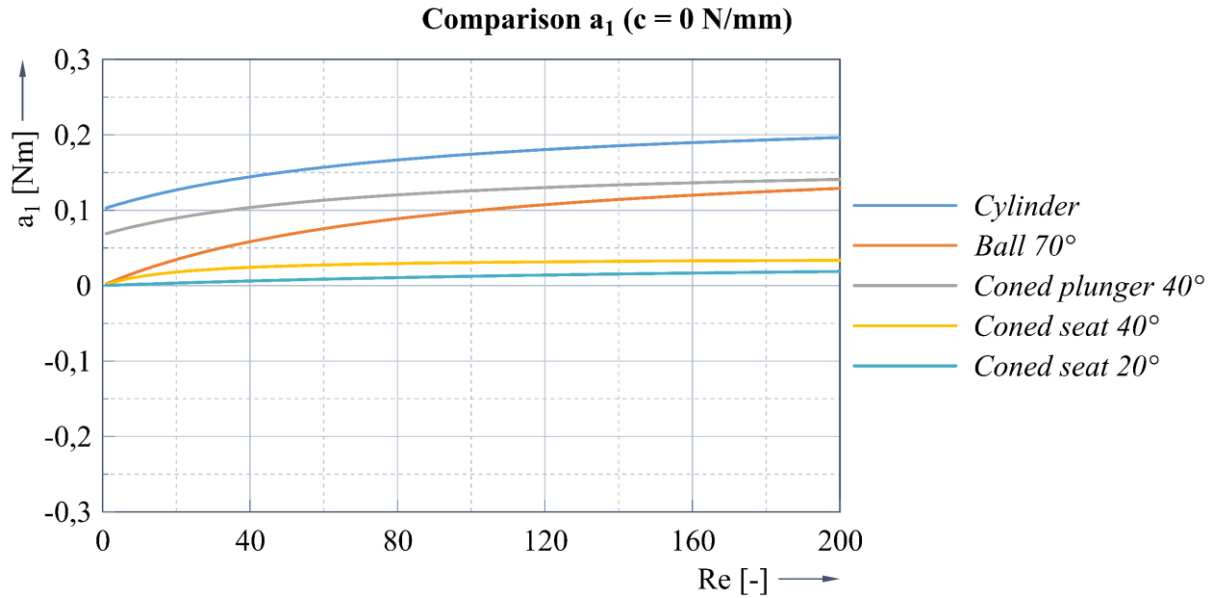
Figure 19: $a_1(c = 0 \frac{N}{mm})$ comparison for the various geometries

This time, as expected, all geometries fulfill the first stability criteria. Now, the second criteria D_2 can be evaluated. Hereby, the viscous damping b is a very important parameter. Usually, the damping should be rather small in order to provide good dynamic valve behavior (e.g. valve shift time). At the same time, reviewing equation (25) shows a minimum viscous damping is required to avoid valve oscillation. Therefore, the equation can be solved for b which leads to a description for the critical damping b_{crit}:

$$b_{crit} = \sqrt{\frac{2F_0}{\rho G_1} \frac{K}{V_A}} \sqrt{\frac{1}{\zeta}} \frac{mG_1{}^2 G_3}{(c_S + c_M)G_1 - F_0 G_2 + 2F_0 G_3 k_{GF} \frac{1}{\zeta}} \tag{28}$$

Using equation (28) the required damping for all geometries can be calculated and compared. Additionally, the influence parameters can be seen, which can help to optimize the system. The different achieved results for the geometries are depictured in **Figure 20** below:

Comparison b_crit (c = 0 N/mm)
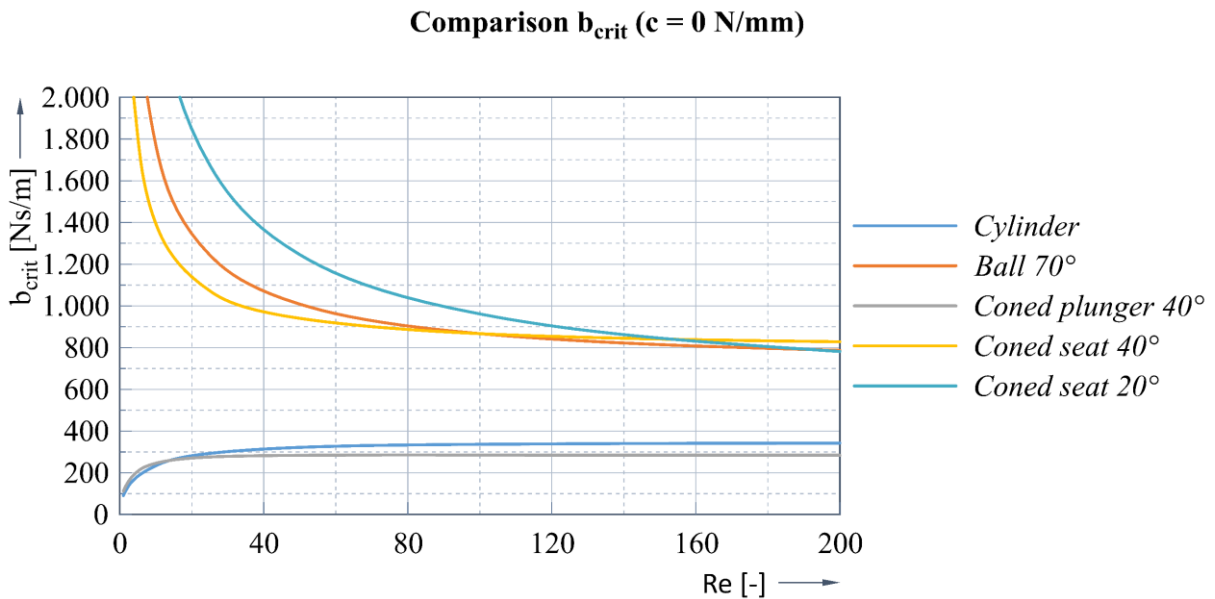
Figure 20: b_{crit} comparison for the various geometries

5. CONCLUSION AND OUTLOOK

In the first section of this paper, the analytical derivation for the different sub-systems of a pilot stage for a two-staged pressure control valve are explained. Several simplifications in form of e.g. linearization of the pressurized area are presumed. The various possibilities for the force-stroke behavior of the electromagnetic actuator are shown and used as influence study later in this paper. Based on the explained equations of the subsystem, the dynamic behavior of the pilot stage is achieved and is described by the force balance (16), pressure equations depending on stroke (20) and finally the differential equation third order of the system (21). The main approach of this paper is to describe and evaluate different possible valve seat geometries.

First, the various characteristics of the geometries were analyzed by the pQx-behavior. Therefore, four different methods can be used: Analytically, CFD-Simulations, 1D-Sytstem simulation, or measurements on samples. However, the goal was to create a manual way with an analytical approach to calculate the pQx-behavior with an acceptable deviation which was achieved. The required geometrical influence parameters can be calculated and compared with the equations (7). The hydraulic resistance is the only parameter which cannot be directly calculated. It was shown that it can be quantified with the equation (27) from CFD-simulation or measurements. The resulting pQx-characteristics of the various geometries shows the different behavior, especially regarding a laminar or turbulent flow. Depending on an industrial usage of the valve, advantages, e.g. regarding higher viscosity influence and with that more temperature dependences can be determined and geometries chosen. The validation of the calculated results has been done by comparing 1D-system simulations, CFD- simulations and test bench measurements.

Secondly, the same geometries of the pilot stage valve seat should be evaluated regarding oscillation tendency. With the explained Routh-Hurwitz method based on equation (21) two main criteria for a_1 (24) and D_2 (26) are shown and the results are depicted. At this point, the analytical approach and the criteria of the equation (24) and (28) help significantly to identify and understand the impact parameters and to evaluate improvements. One further identified influence parameter is the resulting force gradient over stroke, which mainly depends on the magnetic layout. Thereby, the direct relation from the gradient to the function and the oscillation tendency was discovered and verified. This investigation could be extended to focus on the relationship between magnetic force gradient of the actuator and the influence on the performance.

Summarizing this paper, the analytical approach shows in detail the influence parameters which help to understand the performance and the dependencies. This can be used to understand this valve type and should support new developments and improvements on existing applications. In addition, this approach can be repeated by users and a calculation template can be created in a similar way. In general, this investigation should be valid for pilot stages as well as pressure relief valve considering similar boundary conditions.

An extremely important parameter was not considered in this paper: temperature. All the calculations, simulations and measurements have been done at a constant temperature. Especially with a laminar dominant valve design and operation, the temperature has a significant influence due to the viscosity dependency. This approach, which was used and explained in this paper, could be extended by the additional dimension of the temperature. Thereby, different geometrical dependencies for the temperature, overall performance and oscillation tendency could be discovered and quantified.

NOMENCLATURE

A_{flow}	Flow cross section	m^2
A_p	Pressurized area	m^2
a_0, a_1, a_2, a_3	Stability coefficients	
b	Hydraulic damping	Ns/m
b_{crit}	Critcal hydraulic damping	Ns/m
c_{crit}	Critical force gradient	N/m

c_M	Magnetic force gradient	N/m
c_S	Spring stiffness	N/m
d	Diameter	m
d_h	Hydraulic diameter	m
D_0, D_1, D_2	Determinants	
F_{flow}	Flow force	N
F_M	Magnetic force	N
F_p	Pressure force	N
F_S	Spring force	N
F_0	Initial force	N
$G_1,$	Geometrical parameter	m^2
G_2, G_3	Geometrical parameter	m
I	Electrical current	A
k_{GF}	Flow force coefficient	-
K	Bulk modulus	bar
K_1, K_2	Hydraulic resistance constants	-
M	Routh-Hurwitz Matrix	m^2/s
m	Masse	kg
v	Kinematic viscosity	m^2/s
p	Pressure	bar
P	Perimeter	m
Q_{in}	Inlet volume	l/min
Q_{ab}	Outlet volume	l/min
ρ	Density	kg/m^3
Re	Reynolds number	-
t	Time	s
V_A	Chamber volume	m^3
x	Stroke	m
ζ	Hydraulic resistance	-

REFERENCES

[1] Osterland S (2018) Analytical Description of the Static and Dynamic Behaviour of a Pressure Relief Valve. Symposium on Fluid Power and Motion Control FPMC2018. Bath, UK. DOI:10.1115/FPMC2018-8859

[2] Will D, (2008) Hydraulik, Heidelberg, Germany

[3] Wehner, D, (2008) Modellbasierter Systementwurf am Beispiel vorgesteuerter Druckbegrenzungsventile. PhD Thesis, Institute of Fluid Power, Dresden, Germany

[4] Erhard, M, (2016) Regelverhalten, Gestaltdesign und Robustheit direktgesteuerter Proportionaldruck-begrenzungsventile, PhD Thesis, Institute of Fluid Power, Dresden, Germany

[5] Wobben, G, (1978) Statisches und dynamisches Verhalten vorgesteuerter Druckbegrnzungsventile unter besonderer Berücksichtigung der Strömungskräfte, PhD Thesis, Institute of Mechanical Engineering, Aachen, Germany

[6] Schulz, G, (2007) Regelungstechnik 1: Lineare und Nichtlineare Regelung, Rechnergestützter Regelentwurf, München, Germany